The contorted New England Orogen (eastern Australia): New evidence from U-Pb geochronology of early Permian granitoids

Gideon Rosenbaum,[1] Pengfei Li,[1] and Daniela Rubatto[2]

Received 9 June 2011; revised 21 November 2011; accepted 29 November 2011; published 3 February 2012.

[1] A series of sharp bends (oroclines) are recognized in the Paleozoic to early Mesozoic New England Orogen of eastern Australia. The exact geometry and origin of these bends is obscured by voluminous magmatism and is still debated. Here we present zircon U-Pb ages that confirm the lateral continuation of early Permian (296–288 Ma) granitoids and shed new light on the oroclinal structure. Orogenic curvature is defined by the alignment of early Permian granitoids parallel to the structural grain of the orogen, as well as the curved geometry of sub-vertical deformation fabrics, forearc basin terranes, and serpentinite outcrops. Alternative geometrical interpretations may involve two bends (Texas and Coffs Harbour Oroclines), three bends (+Manning Orocline), or even four bends (+Nambucca Orocline). We argue that the model involving four bends is most consistent with available data, although further kinematic constraints are required to confirm the existence of the Manning and Nambucca Oroclines. A subsequent phase of younger magmatism (<260 Ma) cuts across the curved structural grain, providing a minimum age constraint for orocline development. Assuming a structure of four oroclines, we suggest a tentative tectonic model that involves an early stage of subduction curvature during slab rollback at 300–285 Ma, followed by bending associated with dextral transpression. A final tightening of the curved structures was possibly obtained by E-W shortening during the late Permian to Triassic (265–230 Ma) Hunter-Bowen orogeny.

Citation: Rosenbaum, G., P. Li, and D. Rubatto (2012), The contorted New England Orogen (eastern Australia): New evidence from U-Pb geochronology of early Permian granitoids, *Tectonics*, *31*, TC1006, doi:10.1029/2011TC002960.

1. Introduction

[2] Curved mountain chains, commonly referred to as oroclines, have fascinated geologists since the early work by *Carey* [1955], and are still the focus of much research [*Marshak*, 2004; *Sussman and Weil*, 2004; *Van der Voo*, 2004]. Tight curvatures are recognized globally in both modern [*Lonergan and White*, 1997; *Johnston*, 2001; *Ghiglione and Cristallini*, 2007] and ancient [*Kent*, 1988; *Weil et al.*, 2001; *Abrajevitch et al.*, 2007; *Gutiérrez-Alonso et al.*, 2008] orogenic belts. However, the tectonic processes responsible for this curvature are still a matter of debate. Relatively gentle oroclines are common in fold-and-thrust belts (e.g., Appalachians) and are normally restricted to shallow crustal levels [*Marshak*, 1988; *Weil et al.*, 2010]. In contrast, tighter subduction-related bends (e.g., in the Mediterranean Sea), can involve bending and tearing of the whole subducting lithosphere [*Cifelli et al.*, 2007; *Rosenbaum et al.*, 2008]. Tectonic models for the formation of such oroclines have been attributed to rollback of narrow subduction segments accompanied by rotations of crustal blocks around vertical axes [*Kastens et al.*, 1988; *Royden*, 1993; *Rosenbaum and Lister*, 2004; *Cifelli et al.*, 2007], 'escape' tectonics in response to plate convergence [*Mantovani et al.*, 1996] or crustal-scale buckling [*Johnston and Mazzoli*, 2009].

[3] A major challenge is the reconstruction of oroclines in ancient orogenic belts where there are only patchy constraints on the oroclinal structure and related kinematics. Paleozoic oroclines in Variscan Europe and Central Asia have been the subject of structural and paleomagnetic studies that demonstrated the role of block rotations around vertical axes during oroclinal bending [*Weil et al.*, 2000, 2001; *Abrajevitch et al.*, 2007; *Xiao et al.*, 2010]. However, the geodynamic setting associated with these rotations is generally poorly understood. Oroclinal structures have also been described in the Paleozoic to early Mesozoic subduction-related New England Orogen of eastern Australia (Figure 1) [*Cawood and Leitch*, 1985; *Korsch and Harrington*, 1987; *Rosenbaum*, 2010], but there is little agreement regarding the geometry and nature of these oroclines.

[4] The aim of this paper is to unravel the large-scale structure of the New England oroclines, which occur in the

[1]School of Earth Sciences, University of Queensland, Brisbane, Queensland, Australia.
[2]Research School of Earth Sciences, Australian National University, Canberra, ACT, Australia.

Copyright 2012 by the American Geophysical Union.
0278-7407/12/2011TC002960

source: https://doi.org/10.7892/boris.84889 | downloaded: 12.10.2024

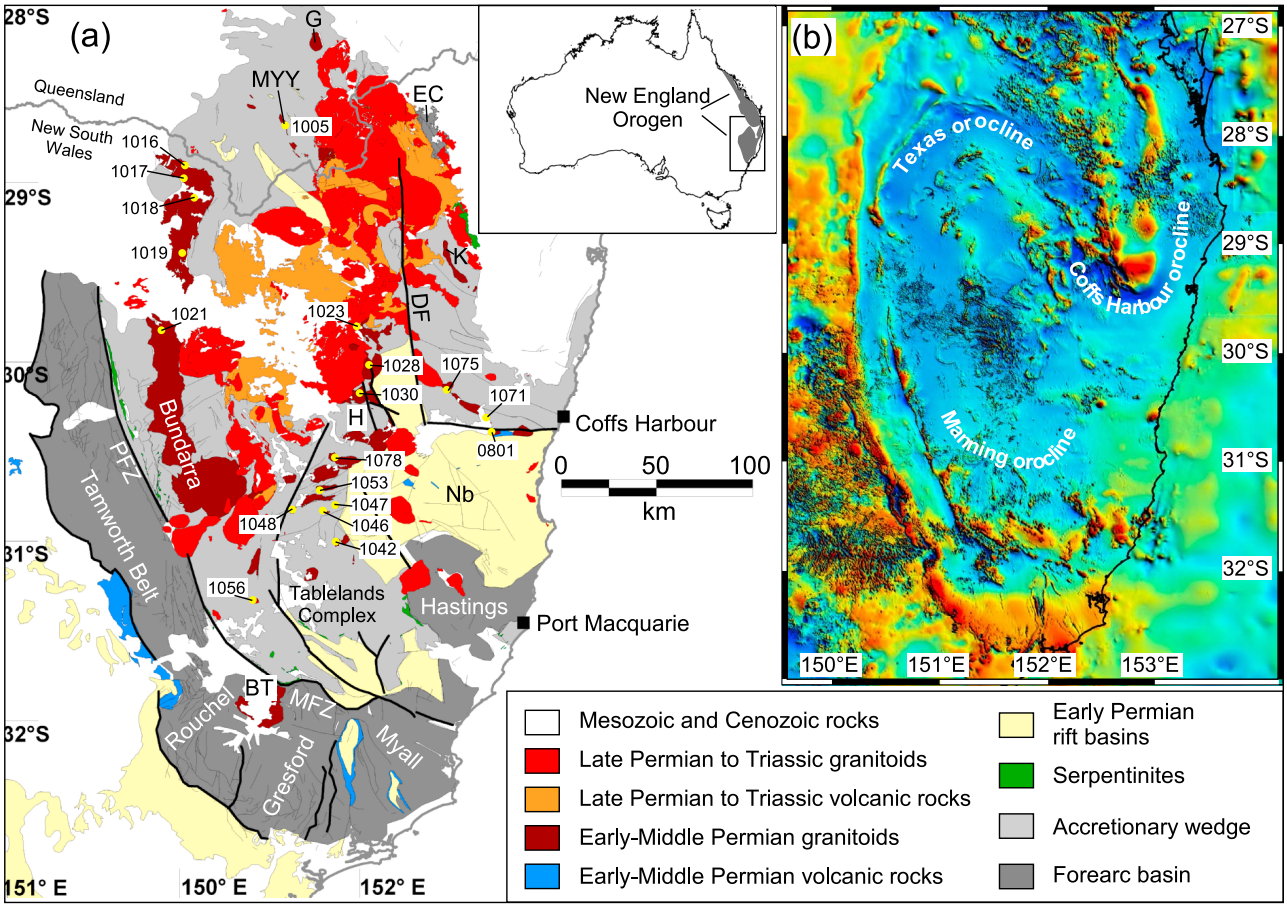

Figure 1. (a) Geology of the southern New England Orogen and sample locations (filled circles). Geological mapping is after 1:250,000 map sheets (Singleton, Newcastle, Tamworth, Hastings, Manilla, Dorrigo-Coffs Harbour, Inverell and Grafton) and 1:100,000 map sheets (Ashford, Clive, Texas, Stanthrope, Drake, Inglewood and Allora). BT, Barrington Tops Granodiorite; DF, Demon Fault; G, Greymare Granodiorite; H, Hillgrove Suite; K, Kaloe Granodiorite; MFZ, Manning Fault Zone; MYY, Mt You You Granite; Nb, Nambucca Block; PFZ, Peel Fault Zone. (b) Total magnetic intensity image of the southern New England Orogen [after *Milligan et al.*, 2010].

southern part of the orogen and are recognized in gravity and magnetic images (Figure 1). Only limited information is known on the kinematics associated with these bends; therefore, the term "orocline" is used here in a general sense as describing orogenic curvature, rather than the strict sense that refers to secondary bending associated with vertical-axis block rotations [*Weil and Sussman*, 2004]. Moreover, some of the structural characteristics defining these bends are ambiguous, and as a result, there are a number of contrasting structural models involving two [*Offler and Foster*, 2008], three [*Korsch and Harrington*, 1987] or four [*Rosenbaum*, 2012] bends. In this paper, we provide a critical evaluation of data supporting oroclinal bending and discuss alternative models for the contorted structure.

[5] The structure of the Texas and Coffs-Harbour Oroclines (Figure 1) define a large (~350 km wide) Z-shaped fold, which according to some authors, formed in response to a N-S dextral transform boundary [*Murray et al.*, 1987; *Offler and Foster*, 2008]. The existence of a third orocline farther south, the Manning Orocline is less clear in geophysical images (Figure 1b), but has been advocated by some authors based on the arcuate shape of a serpentinite belt and paleomagnetic data from rotated forearc basin terranes (Figure 1a) [*Cawood and Leitch*, 1985; *Korsch and Harrington*, 1987; *Geeve et al.*, 2002; *Glen*, 2005; *Klootwijk*, 2009; *Cawood et al.*, 2011b]. Other workers have considered this evidence as tenuous, arguing that no significant data support the existence of the Manning Orocline [*Offler and Foster*, 2008]. We demonstrate that the spatial distribution of early Permian (Cisuralian) granitoids from the southern New England Orogen is a marker that defines the oroclinal structure. We present new SHRIMP U-Pb ages, and show that a number of granitic suites, which were previously considered to represent two episodes of magmatism, were in fact emplaced simultaneously over a short time interval at 296–288 Ma. The contorted lateral continuation of these granitoids suggests an oroclinal structure that is far more complex than previously recognized.

2. Geological Setting

[6] The New England Orogen is the youngest and easternmost component of the Tasmanides orogenic collage of eastern Australia [*Glen*, 2005]. It occupied a supra-

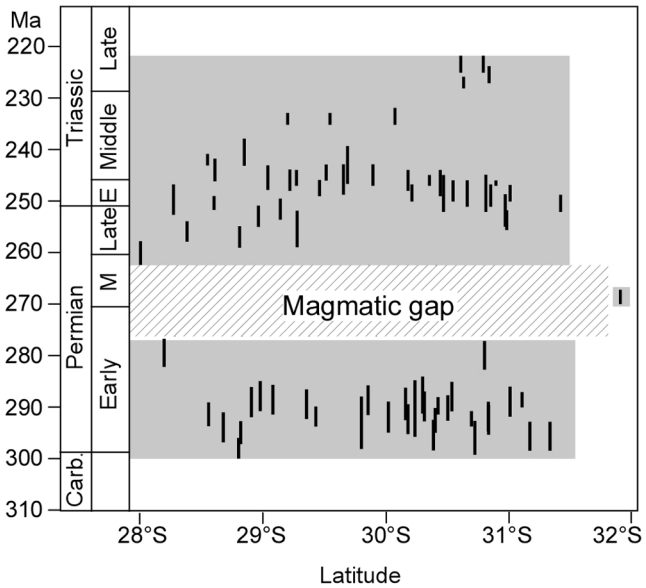

Figure 2. Diagram showing the timing of magmatism in the southern New England Orogen based on published data [*Shaw*, 1994; *Bryant et al.*, 1997b; *Kleeman et al.*, 1997; *Vickery et al.*, 1997; *Donchak et al.*, 2007; *Cross et al.*, 2009; *Cawood et al.*, 2011b].

subduction position from the Late Devonian to the Early Triassic, as indicated by the occurrence of Devonian to Carboniferous volcanic arc, forearc basin and accretionary wedge rocks, as well as a large volume of Permo-Triassic magmatic rocks [*Leitch*, 1974; *Murray et al.*, 1987].

[7] The oroclines are found in the southern part of the New England Orogen. The majority of the rocks in this area record a Devonian-Carboniferous west-dipping subduction zone represented by forearc basin and accretionary wedge rocks (Figure 1a, Tamworth Belt and Tablelands Complex, respectively). The Devonian-Carboniferous volcanic arc is found farther west, but is predominantly covered by younger sedimentary rocks [*McPhie*, 1987].

[8] The Tamworth Belt is characterized by an arc-related basin fill, which was deposited on a shelf that was gradually deepening from west to east [*Crook*, 1964; *Roberts and Engel*, 1987]. Correlative stratigraphic successions are found in a number of, supposedly displaced, forearc basin terranes (Emu Creek, Rouchel, Gresford, Myall and Hastings Blocks; Figure 1a), with the Hastings Blocks showing water deepening from east to west [*Lennox and Roberts*, 1988], i.e., opposite to the sense of sedimentation in the Tamworth Belt.

[9] Rocks in the Tablelands Complex are typically deep marine volcaniclastic turbidites and cherts, mafic volcanic rocks, and olistostromal deposits [*Leitch and Cawood*, 1980; *Cawood*, 1982; *Fergusson*, 1984]. These rocks were subjected to varying metamorphic conditions (from prehnite-pumpellyite/lower greenschist to amphibolite-facies), and are characterized by a penetrative steeply dipping structural fabric [*Binns et al.*, 1967; *Korsch*, 1981; *Dirks et al.*, 1992; *Li et al.*, 2012].

[10] The boundary between the Tamworth Belt and the Tablelands Complex is a tectonic contact, the Peel-Manning Fault System (Figure 1a), which is characterized by exposures of serpentinites, blueschists and eclogites. The age of high-pressure metamorphism is middle Ordovician [*Fukui et al.*, 1995], indicating that this suture is most likely a recycled component of the Lachlan Orogen [*Glen*, 2005].

[11] Early Permian rocks in the southern New England Orogen seem to indicate a major change in the tectonic setting, possibly associated with eastward subduction rollback [*Jenkins et al.*, 2002]. This is indicated by evidence for early Permian backarc extension [*Korsch et al.*, 2009a], and the occurrence of S-type, possibly backarc-related, magmatism in the former forearc region [*Shaw and Flood*, 1981]. The geodynamic setting of S-type magmatism has been discussed by *Collins and Richards* [2008], who suggested that S-type granites in eastern Australia were associated with episodic subduction rollback, with their emplacement heralding the formation of backarc extensional basins. The emplacement of S-type granitoids in the southern New England Orogen occurred simultaneously with the development of rift basins filled with clastic sedimentary rocks (e.g., Nambucca Block, Figure 1a) and bimodal volcanism [*Asthana and Leitch*, 1985; *Leitch*, 1988; *Caprarelli and Leitch*, 2001].

[12] Early Permian (300–285 Ma) granitoids were emplaced in two major suites, the S-type Bundarra Granite and the Hillgrove Suite, and in a number of other smaller S- and I-type plutons (e.g., Mt You You Granite, Kaloe Granodiorite; Figure 1a). Earlier publications, mainly based on Rb-Sr geochronology, have considered ages of 290–280 Ma for the Bundarra Granite and 310–300 Ma for the Hillgrove Suite [*Flood and Shaw*, 1977; *Mensel et al.*, 1985; *Collins et al.*, 1993; *Kent*, 1994]. However, recent U-Pb zircon ages [*Cawood et al.*, 2011b] and results of this study show that the two S-type suites were emplaced simultaneously at 296–288 Ma. The I-type Kaloe Granodiorite has recently been dated at 292 Ma [*Cawood et al.*, 2011b].

[13] Following the first stage of magmatism in the early Permian, the southern New England Orogen experienced a long period with scarce magmatism (~285–260 Ma, Figure 2). The only known granitoids of these ages are the Barrington Tops Granodiorite (267 Ma [*Cawood et al.*, 2011b]) and Greymare Granodiorite (280 Ma [*Donchak et al.*, 2007]), located in the southern and northern parts of the southern New England Orogen, respectively (Figure 1a). The end of the magmatic gap coincides with the onset of ~E-W contractional deformation, locally known as the Hunter-Bowen orogeny [*Collins*, 1991; *Holcombe et al.*, 1997b; *Korsch et al.*, 2009b], which commenced at ~265 Ma and continued until ~230 Ma. This deformation involved westward-propagating retro-thrusting of the early Permian rift basins, which evolved into foreland systems [*Fergusson*, 1991; *Korsch et al.*, 2009b]. In the southern New England Orogen, deformation during the Hunter-Bowen Orogeny affected early Permian sedimentary rocks of the Nambucca Block (Nb in Figure 1a), giving rise to the development of penetrative ductile fabrics [*Johnston et al.*, 2002; *Offler and Foster*, 2008].

[14] A second stage of Permian-Triassic magmatism occurred at 260–220 Ma and was partly overlapped with the Hunter-Bowen orogeny (Figure 2). It produced voluminous I-type granitoids and calc-alkaline volcanic rocks, which

were supposedly emplaced in a continental subduction arc setting [*Flood and Shaw*, 1975; *Bryant et al.*, 1997a].

3. Geochronology

3.1. Sampling Locations

[15] Sampling was targeted to obtain precise age constraints on the timing of emplacement of early Permian granitic plutons. We analyzed samples from 19 different localities across the entire southern New England Orogen (Figure 1a). Sampling was particularly close-spaced within the Bundarra and Hillgrove Suites, with the addition of a few other isolated bodies to complete the profile. For a lithological description of all samples, see Table 1.

[16] Sample NE1005 is from Mt You You Granite, which is a narrow and elongated (~14 km long) intrusion in the eastern limb of the Texas Orocline. The pluton is characterized by a relatively heterogeneous composition associated with biotite monzogranite, syenogranite and minor hornblende-biotite monzogranite. In the sampling location, the granite incorporates mafic enclaves, and is weakly deformed as indicated by a spaced foliation. The sample analyzed is granitic in composition, consisting of medium grained K-feldspar, quartz, plagioclase and minor biotite and chlorite.

[17] Samples NE1016, NE1017, NE1018, NE1019 and NE1021 were taken from five different localities within the Bundarra Granite. All five samples are characterized by a roughly similar mineral composition, consisting of large K-feldspar phenocrysts (1–2 cm), plagioclase, quartz and biotite.

[18] The majority of analyzed samples were taken from plutons of the Hillgrove Suite, which is subdivided into two sectors, a western sector of intrusions oriented roughly N-S in the central part of the study area, and an eastern sector oriented NW-SE west of Coffs Harbour (Figure 3a). Within these two sectors two other granitic plutons, termed here the Rockisle Granite and Gandar Granodiorite, were also sampled. Ten samples were analyzed from the western sector, which included S-type monzogranites (NE1048, NE1046, NE1053, NE1078, NE1030 and NE1028), granodiorite (NE1042), granites (NE1056 and NE1023), and diorite (NE1047 from the Cheyenne Complex). Many of these plutons are internally deformed by localized ductile shear zones and spaced foliation. Three samples were analyzed from the eastern sector, which included S-type granodiorites (NE1075 and NE1071) and a diorite (NE0801).

3.2. Methodology

[19] Zircon grains were separated after rock crushing using conventional heavy liquid and magnetic properties. The grains were mounted in epoxy resin and polished to expose a near equatorial section. Cathodoluminescence (CL) investigation was carried out on two different scanning electron microscope supplied with an ellipsoidal mirror for CL at the Australian National University in Canberra: a HITACHI S2250N and a JEOLJSM-6610A operating at similar conditions of 15 kV and 20 mm working distance.

[20] The zircons were analyzed for U, Th and Pb using the sensitive high resolution ion microprobes (SHRIMP II and SHRIMP RG) at the Australian National University. Instrumental conditions and data acquisition are described by *Williams* [1998]. The data were collected in sets of six scans throughout the masses and a reference zircon was analyzed each fourth analysis. U-Pb data were collected over several analytical sessions using the same standard, with analytical sessions having calibration errors between 1.4 and 2.5% (2 sigma), which was propagated to single analyses. The measured $^{206}Pb/^{238}U$ ratio was corrected using reference zircon from the Temora granodiorite (TEM) [*Black et al.*, 2003]. The analyses were corrected for common Pb using three different methods based on ^{204}Pb, ^{207}Pb and ^{208}Pb following *Williams* [1998]. All three corrections returned results identical within error. The common Pb composition was assumed to be that predicted by the *Stacey and Kramers* [1975] model. We present data on Concordia diagrams based on the ^{204}Pb or ^{208}Pb common Pb correction and report weighted mean $^{206}Pb/^{238}U$ ages at 95% confidence level (c.l.) and relative MSWD, after exclusion of outliers. In most samples the average $^{206}Pb/^{238}U$ ages, which typically have a 0.5–0.7% error (95% c.l.) are forced to 1% to account for external errors. Data evaluation and age calculation were done using the software Squid 1 and Isoplot/Ex [*Ludwig*, 2003].

3.3. Results

[21] Zircon crystals separated from all samples are euhedral and generally elongated, as typically observed in felsic granitic rocks. Their internal structure is characterized by oscillatory zoning (Figure S1 in the auxiliary material).[1] In most samples, a percent of crystals contains cores with zoning that is truncated by the oscillatory zoning of the rim. U-Pb analyses (Tables S1–S19 in Text S1 in the auxiliary material) were concentrated on the zircon rims. They systematically yielded reproducible ages, and their averages were taken as the age of granite crystallization (Figure S2).

[22] In most samples, a few analyses on grain cores returned significantly older ages (335–304 Ma), indicating an inherited nature of the cores. Notably, some cores are only marginally younger than the main zircon population and could thus represent early product of the same magmatic system. Analyses returning apparent ages younger than the main population are present in six samples and correspond to crystal rims. Such analyses are interpreted as localized disturbance of the U-Pb system and were excluded from the age calculation. Discordant analyses were also excluded when calculating average ages.

[23] Average ages of all samples (Table 1 and Figure S2) indicate that the granitoids belong to the first episode of Permian magmatism (Figure 2). The oldest components of this magmatism (~296–294 Ma) are represented by the Mt You You Granite, the Rockisle Granite, the Blue Knobby Monzogranite and the Dorrigo Mountain Complex (Figure 3). The five samples from the Bundarra Granite yielded consistent ages from 287.9 ± 2.9 to 289.5 ± 2.9. Samples from the Bundarra and the Hillgrove largely overlap in age. The dioritic sample from the Cheyenne Complex yielded a significantly younger age of 280.0 ± 2.8 Ma.

4. Tectonic Implications: The Contorted Early Permian Magmatic Belt

[24] Our geochronological data indicate that magma emplacement within a relatively narrow belt that follows the

[1]Auxiliary materials are available in the HTML. doi:10.1029/2011TC002960.

Table 1. Sample Locations, Lithological Characteristics and U-Pb Zircon Ages

Sample Number	Suite	Rock Unit	Description	Mineralogical Assemblage	Latitude	Longitude	$^{206}Pb/^{238}U$ Age (Ma)	MSWD	Number of Analyses
NE1005	Mount You You	Mount You You Granite	Granite. Fine to medium-grained and pale color	K-feldspar, quartz, plagioclase, biotite and chlorite	−28.675	151.581	294.0 ± 2.9	2.4	24/27
NE1016	Bundarra	Bundarra Granite	Granite. Medium to coarse grained	K-feldspar phenocrysts (1–2 cm), plagioclase, quartz and biotite	−28.902	151.029	289.1 ± 2.9	1.7	19/21
NE1017	Bundarra	Bundarra Granite	Granite. Medium to coarse grained	K-feldspar phenocrysts (1–2 cm), plagioclase, quartz and biotite	−28.970	151.022	287.9 ± 2.9	1.3	18/23
NE1018	Bundarra	Bundarra Granite	Granite. Medium to coarse grained	K-feldspar phenocrysts (1–2 cm), plagioclase, quartz and biotite	−29.082	151.080	288.6 ± 2.9	2.2	18/22
NE1019	Bundarra	Bundarra Granite	Granite. Medium to coarse grained	K-feldspar phenocrysts (1–2 cm), plagioclase, quartz and biotite	−29.391	151.015	289.5 ± 2.9	1.6	23/25
NE1021	Bundarra	Bundarra Granite	Granite. Medium to coarse grained	K-feldspar phenocrysts (1–2 cm), plagioclase, quartz and biotite	−29.825	150.897	288.7 ± 2.9	3.5	20/24
NE1056	N/A	Rockisle Granite (new name)	Granite. Coarse grained and buff to pink color	K-feldspar, quartz, plagioclase and biotite	−31.337	151.406	294.9 ± 2.9	1.3	17/18
NE1048	Hillgrove	East Lake Monzogranite	Biotite Monzogranite. Foliated, fine grained and equigranular	K-feldspar, quartz, plagioclase, biotite and amphibole (retrogressed)	−30.831	151.631	292.1 ± 2.9	1.4	11/18
NE1042	Hillgrove	Moona Plains Complex	Granodiorite. Fine to medium grained	Feldspar, quartz, amphibole and biotite	−31.007	151.873	289.0 ± 2.9	2.9	17/18
NE1046	Hillgrove	Winterbourne Monzogranite	Monzogranite. Medium grained, buff color and porphyritic texture	Quartz, K-feldspar, plagioclase and minor amphibole	−30.835	151.801	292.5 ± 2.9	2.6	18/19
NE1047	Hillgrove	Cheyenne complex	Diorite. Medium grained	Amphibole (retrogressed), plagioclase, and minor quartz and biotite	−30.802	151.869	280.0 ± 2.8	0.72	15/15
NE1053	Hillgrove	Blue Knobby Monzogranite	Biotite Monzogranite. Medium grained, buff color and equigranular texture	K-feldspar, plagioclase, quartz and biotite	−30.720	151.783	296.0 ± 3.3	2.3	9/14
NE1078	Hillgrove	Hillgrove Monzogranite	Biotite monzogranite. Coarse grained, pink color, granular texture	K-feldspar, plagioclase, quartz and biotite	−30.535	151.869	288.0 ± 2.9	1.6	14/15
NE1030	Hillgrove	Tobermory Monzogranite	Monzogranite. Coarse grained and pink color	Orthoclase, microcline, plagioclase, quartz and biotite	−30.178	152.005	292.4 ± 2.9	2.6	17/19
NE1028	Hillgrove	Kookabookra Monzogranite	Monzogranite. Space foliated, pale to buff color and porphyritic texture	Plagioclase, K-feldspar, quartz and biotite	−30.019	152.059	292.0 ± 3.0	1.3	13/14
NE1023	Hillgrove	Henry River Granite	Granite. Strongly foliated and fine grained	K-feldspar, quartz and minor biotite	−29.802	151.990	293.1 ± 5.1	0.07	3/7
NE1075	Hillgrove	Sheep Station Creek Complex	Granodiorite. Medium grained and deformed	Quartz, feldspar, and abundant of mafic minerals	−30.160	152.491	289.4 ± 3.1	1.4	14/15
NE1071	N/A	Gandar Granodiorite (new name)	Granodiorite. Coarse to very coarse grained, pale color and porphyritic texture	Large plagioclase phenocrysts (0.5–1.5cm), quartz and biotite	−30.313	152.715	290.9 ± 2.9	1.7	15/19
NE0801	Hillgrove	Dorrigo Mountain Complex	Diorite. Medium grained and dark colour	Amphibole (retrogressed), feldspar, quartz and minor biotite	−30.394	152.745	295.5 ± 3.0	1.3	23/23

shape of the oroclines occurred at 296–288 ± 3 Ma (Figure 3a). The oroclines can be defined by the lateral continuation of this magmatic belt (Figures 3b–3d). In the north, the western limb of the Texas Orocline is defined by the northern part of the Bundarra Granite (290–288 ± 3 Ma). The continuation of the oroclinal structure is recognized in a series of internally deformed S-type granites, dated at ~298–291 Ma and oriented parallel to the eastern limb of the Texas Orocline (Bullanganag, Mt You You, Ballandean, and Jibbinbar; Figure 3a). Farther east, the ~292 Ma Kaloe Granodiorite [*Cawood et al.*, 2011b] is interpreted as the eastern continuation of this belt (Figures 3b and 3c).

[25] One of the most important implications of the geochronological data is that magma emplacement in the

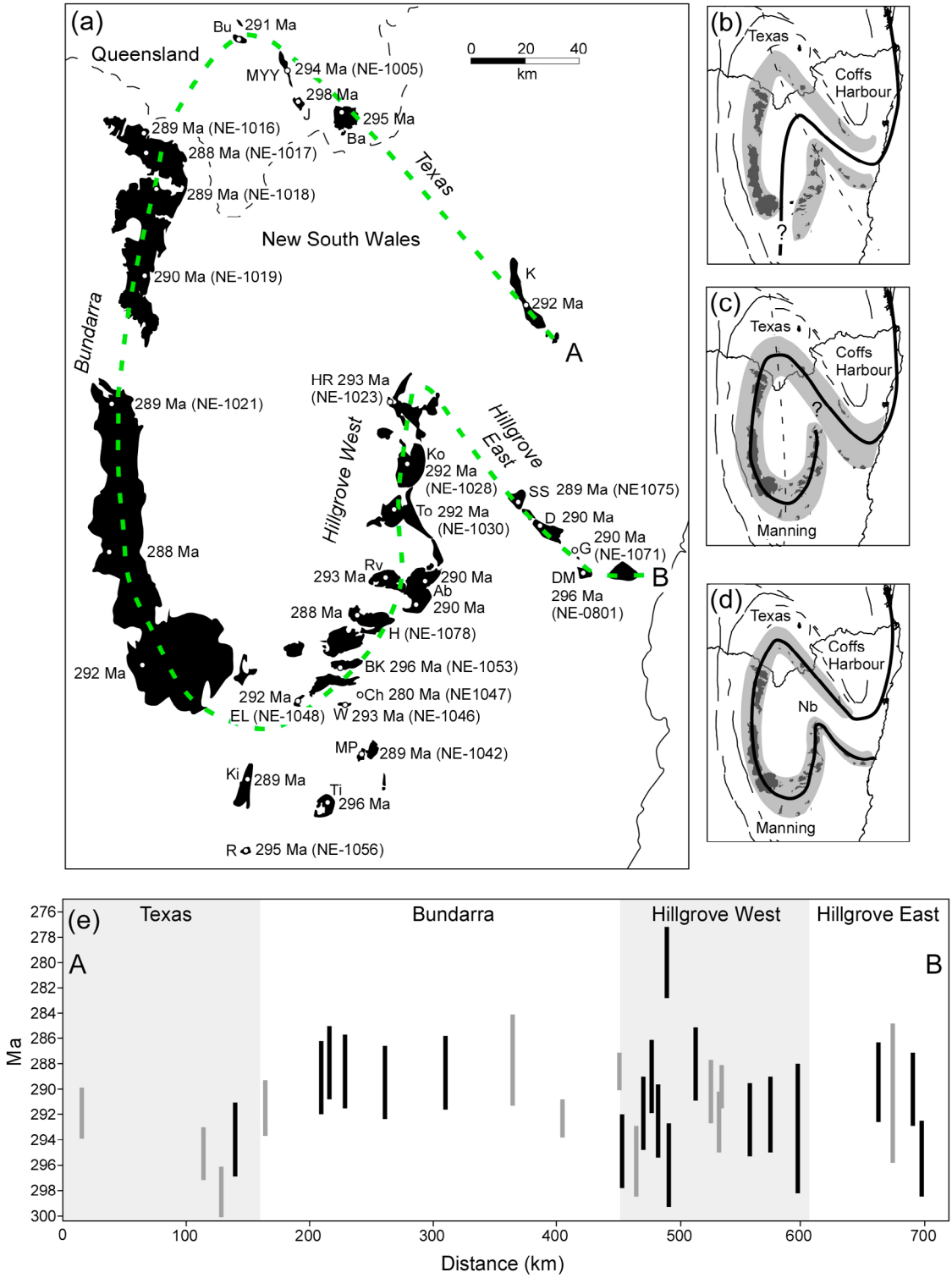

Figure 3

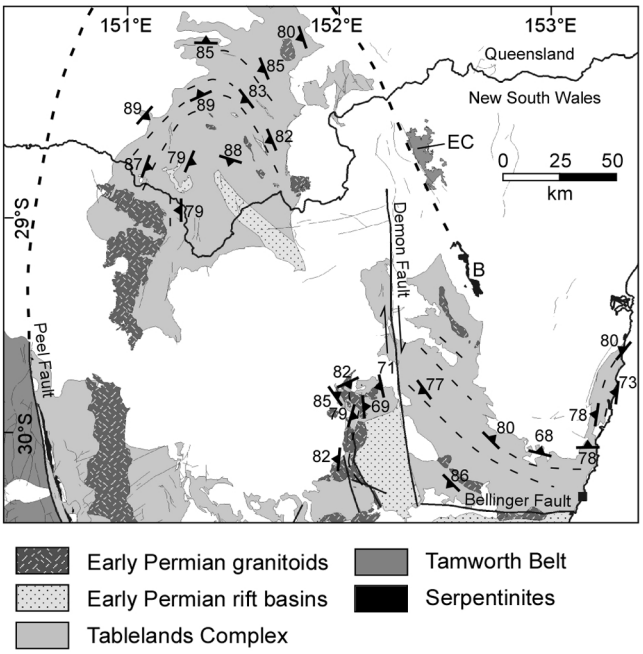

Figure 4. Map showing Devonian to early Permian rocks around the Texas, Coffs Harbour and Nambucca Oroclines and orientations of the dominant structural fabrics (thin dashed line). Structural data are taken from *Li et al.* [2012] (Texas Orocline), *Korsch* [1981] (Coffs Harbour Orocline) and *Moule* [2011] (Nambucca Orocline). B, Baryulgil Serpentinite; EC, Emu Creek Block.

Bundarra (290–288 Ma) and Hillgrove (296–288 Ma) Suites took place during a relatively short time interval lasting approximately ~10 Ma. The only exception is the Cheyenne Complex in the Hillgrove Suite, for which we obtained a younger age of 280.0 ± 2.8 Ma. A number of other samples from the Hillgrove Suite yielded identical ages to those obtained in the Bundarra Granite (e.g., Moona Plains Complex 289.0 ± 2.9 and Hillgrove Monzogranite 288.0 ± 2.9). Accordingly, we propose that this belt of contemporaneous magmatism defines the inner hinge of the Manning Orocline (Figures 3c and 3d).

[26] The emplacement ages of granitoids from the eastern part of the Hillgrove Suite (296–289 Ma) demonstrate that the early Permian magmatic belt continues farther east. These plutons are aligned NW-SE, parallel to the Kaloe Granodiorite. Three alterative interpretations can explain these relationships (Figures 3b, 3c, and 3d): (1) the eastern Hillgrove plutons and the Kaloe Granodiorite are parts of two parallel, but unrelated, magmatic belts (Figure 3b); (2) the eastern Hillgrove plutons, together with the Kaloe Granodiorite form a broad magmatic belt surrounding the Coffs Harbour Orocline (Figure 3c); and (3) the two parallel magmatic belts are part of a continuous belt, which is curved around the Texas, Manning and a fourth orocline, which we term here the Nambucca Orocline (Nb in Figure 3d). The first model, which assumes that the Manning Orocline does not exist, cannot explain the southward convergence of the two belts (see question mark in Figure 3b). The second model implies an abrupt and unexplained termination of the early Permian granitoids north of the plutons of the Hillgrove Suite (indicated by a question mark in Figure 3c). The third model explains the lateral continuity of early Permian granitoids and implies a strongly contorted structure of four bends (Figure 3d). As discussed below, we think that this model is most consistent with structural observations.

5. Supporting Structural Data

[27] Structural information from the New England oroclines is relatively patchy due to limited exposures of pre-oroclinal strata, poor outcrop conditions, and extensive coverage of younger sedimentary and magmatic rocks. The available structural evidence is consistent with the oroclinal structure, particularly in the Texas and Coffs Harbour Oroclines.

[28] One of the most important observations is that within the Tablelands Complex, structural fabrics (bedding and secondary foliations) are ubiquitously steeply dipping or sub-vertical (Figures 4 and 5). This may suggest that the recognized map-view curved patterns are real bends around vertical axes rather than projections of shallow dipping structures intersecting the topography. Alternatively, it is possible that the steep curved patterns resulted from fold interference. The superposition of upright ~N-S and ~E-W trending folds, for example, could potentially produce similarly curved patterns (Figure 6c). However, no evidence for such interference patterns has been found in mesoscale structures.

Figure 3. (a) Map showing the spatial distribution of early Permian granitoids and their inferred contorted structure (thick dashed line). U-Pb SHRIMP ages are based on results of this study, complemented by data from *Donchak et al.* [2007] (Bu), *Cross et al.* [2009] (J), *Cawood et al.* [2011b] (two samples from the southern Bundarra Granite, K, Ab, Rv, D, Ti and Ki), and an unpublished age from Geoscience Australia (Ba). Ab, Abroi Granodiorite; Ba, Ballandean Granite; BK, Blue Knobby Monzogranite; Bu, Bullaganang Granite; Ch, Cheyenne complex; D, Dundurrabin Granodiorite; DM, Dorrigo Mountain Complex; EL, East lake Monzogranite; G, Gandar Granodiorite; H, Hillgrove Monzogranite; HR, Henry River Monzogranite; J, Jibbinbar Granite; K, Kaloe Granodiorite; Ki, Kilburnie Monzogranite; Ko, Kookabookra Granodiorite; MP, Moona Plains Complex; MYY, Mt You You Granite; R, Rockisle Granite; Rv, Rockvale Granodiorite; SS, Sheep Station Creek Complex; Ti, Tia Granodiorite; To, Tobermory Monzogranite; W, Winterbourne Monzogranite. Alternative interpretations for the lateral continuation of the early Permian belt, involving (b) two oroclines (Texas and Coffs Harbour), (c) three oroclines (Texas, Coffs Harbour and Manning), and (d) four oroclines (Texas, Coffs Harbour, Manning and Nambucca). Nb, Nambucca Orocline. Bold lines indicate alternative traces of the oroclinal structure and dashed lines indicate axial plane orientations. (e) Timing of early Permian magmatism based on our data (black bars) and published data (gray bars). Localities are projected along the contorted dashed line (A-B in the map) and appear in the horizontal axis as the distance from the Kaloe Granodiorite.

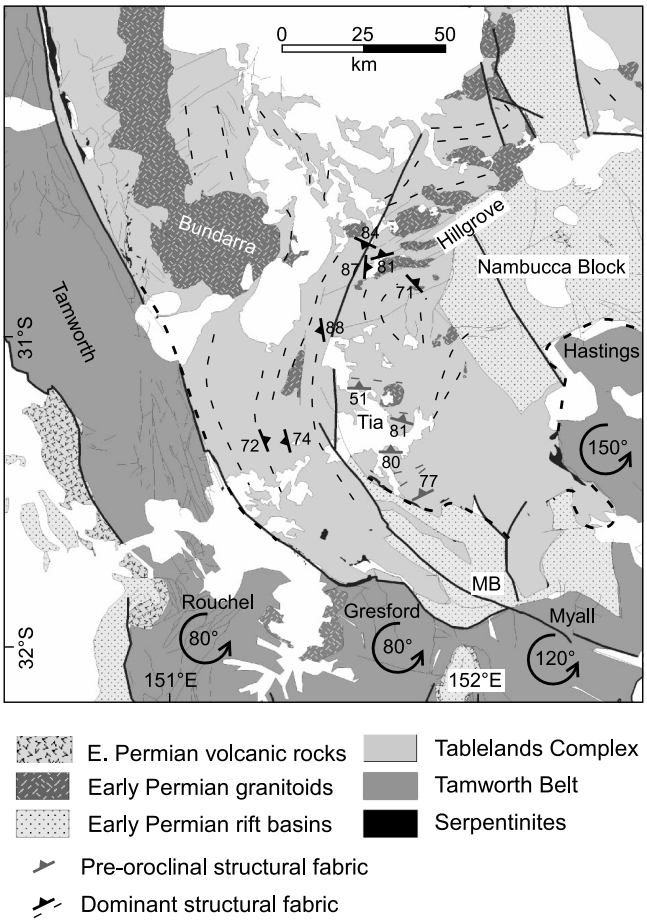

Figure 5. Geological map of the southernmost New England Orogen in the area of the Manning Orocline. The orocline is defined by the arrangement and block rotations of forearc basin terranes, the curvature of the serpentinite belt (thick dashed line) and the curved shape of the early Permian granitoids. Thin dashed lines indicate dominant trends of secondary foliations, possibly comprising a combination of syn- and post-oroclinal ~N-S fabrics and pre-oroclinal fabrics (e.g., E-W orientations in the Tia complex). Fabric elements are based on our own observations, complemented by data from *Binns et al.* [1967] and *Dirks et al.* [1992]. Paleomagnetic block rotations are after *Geeve et al.* [2002] (Rouchel, Gresford and Myall Blocks) and *Klootwijk* [2009] (Hastings Block). MB, Manning Basin. Legend is similar to Figure 4.

[29] In the Texas and Coffs Harbour Oroclines, a dominant structural fabric defined by slaty cleavage is recognized within the accretionary wedge rocks of the Texas Beds and Coffs Harbour Association (Figure 4). This fabric, which is generally sub-parallel to bedding, is aligned parallel to the oroclinal structure [*Korsch*, 1981; *Lennox and Flood*, 1997; *Li et al.*, 2012]. It is considered, therefore, as a pre-oroclinal fabric, which was most likely generated within the accretionary wedge during the Carboniferous [*Graham and Korsch*, 1985]. In the area of the Texas Orocline, a local overprinting fabric parallel to the axial plane of the orocline is recognized but is not penetrative, indicating that the overall strain associated with oroclinal bending was relatively low (<30% shortening) [*Li et al.*, 2012]. N-S-trending mesoscopic folds in the area of the Coffs Harbour Orocline were interpreted by *Korsch* [1981] as pre-oroclinal folding because of their varying orientations across the oroclinal structure. Similarly to the deformation in the Texas Orocline, syn-oroclinal overprinting structures in the Coffs Harbour Orocline are not well developed.

[30] In addition to the curved geometry of the sub-vertical structural fabrics, the existence of the Texas and Coffs-Harbour Oroclines is supported by a number of additional observations. First, the forearc basin exposed in the southern part of the western limb of the Texas Orocline (Tamworth Belt), is represented in the eastern limb by the Emu Creek Block (Figure 4), which is characterized by a comparable Carboniferous tectonostratigraphy [*Cross et al.*, 1987]. Second, the exposure of a serpentinite block in the eastern limb of the Texas Orocline, the Baryulgil Serpentinite (Figure 4), is consistent with the curvature of the serpentinite belt around the orocline. Third, magnetic fabric results show an increase in the intensity of deformation toward the hinges of the oroclines, supposedly in response to oroclinal deformation [*Aubourg et al.*, 2004].

[31] New structural data from the hinge of the Nambucca Orocline is consistent with the curved geometry [*Moule*, 2011], although further structural investigation is required. Steeply dipping dominant structural fabric is curved around the orocline (Figure 4), and locally, there is an overprinting NW-SE secondary fabric parallel to the axial plane of minor folds. A spaced cleavage that follows the curvature of the Nambucca Orocline is also recognized in the early Permian (~293 Ma) Henry River Granite.

[32] Evidence supporting the structure of the Manning Orocline is the curved arrangement of forearc basin terranes and the curvature of the serpentinite belt (Figure 5). Paleomagnetic constraints on vertical-axis block rotations are incomplete [*Cawood et al.*, 2011a]. However, available data from the forearc basin terranes (Rouchel, Gresford and Myall Blocks) are consistent with oroclinal bending, showing increasing amounts of counterclockwise block rotations (80°, 80° and 120°, respectively) [*Geeve et al.*, 2002]. In the Hastings Block, in contrast, *Schmidt et al.* [1994] interpreted 130° clockwise rotation relative to the Australian craton, which is inconsistent with oroclinal bending. However, *Klootwijk* [2009] has recently reinterpreted these paleomagnetic data by comparing the Namurian (326–313 Ma) paleopole with the northern Tamworth Belt, suggesting a 150° counterclockwise rotation. These results are compatible with a model for oroclinal bending (see section 6.3 and Figure 7).

[33] One of the major problems with the interpretation of the Manning Orocline is that bedding and secondary foliations are predominantly oriented N-S (Figure 5). Curved structural fabric is only vaguely recognized in the eastern limb (Figure 5), whereas the dominant ~N-S fabric seems to represent syn-oroclinal deformation parallel to the axial plane of mesoscopic folds. The hinge of the Manning Orocline, in the area of Tia metamorphic complex, is a high-grade zone associated with the emplacement of the Tia Granodiorite [*Dirks et al.*, 1992; *Dirks et al.*, 1993]. The latter has been emplaced at ~296 Ma [*Cawood et al.*, 2011b], and was synchronous with the development of a dominant structural ~N-S fabric [D5 of *Dirks et al.*, 1992].

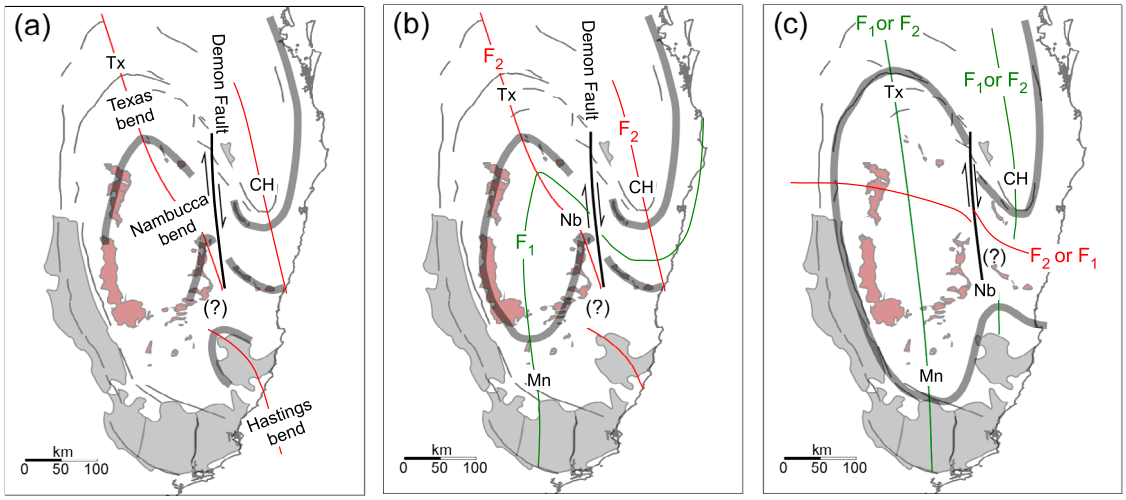

Figure 6. Alternative models for the geometry of the New England oroclines (thick gray line). The spatial distribution of forearc basin terranes (gray) and early Permian granitoids (brown) is shown in the background. Major magnetic lineaments (Figure 1b) are also shown. (a) A two-orocline structure of the Texas and Coffs Harbour Oroclines (see also Figure 3b). Note that bending in the Nambucca and Hastings regions is interpreted here as the southwestward continuation of the axial plane of the Texas Orocline (red), which was possibly affected by post-Triassic strike-slip faulting. (b) A geometrical model for four oroclines showing an early generation Manning Orocline (F_1) folded around NW-SE F_2 folds. (c) An alternative four-orocline geometrical model showing the interference of two orthogonal fold hinges.

An earlier pre-magmatic, and possibly pre-oroclinal, fabric (D4) is oriented E-W [*Dirks et al.*, 1992], i.e., perpendicular to the axial plane of the orocline (Figure 5).

6. Discussion

6.1. How Many Oroclines?

[34] The exact geometry of the oroclinal structure remains controversial and warrants additional structural and kinematic constraints. In particular, structural observations from the hinges of the Manning and Nambucca Oroclines are relatively scarce and/or ambiguous. Therefore, our suggestion that these areas represent major orogenic curvatures should be tested in future studies. The proposed four-orocline structure is consistent with available data and is used here as the basis for our tectonic reconstruction (Section 6.3). We note, however, that alternative geometrical models (Figures 3b–3c) cannot be ruled out.

[35] In a two-orocline model [e.g., *Offler and Foster*, 2008], the Nambucca Orocline can be considered as the inner hinge of the Texas Orocline (Figure 3b). A slightly modified version of this interpretation is illustrated in Figure 6a, showing that the axial plane of the Texas-Nambucca orocline is curved, possibly in response to the post-Triassic dextral offset (20–25 km) along the Demon Fault [*Korsch et al.*, 1978; *McPhie and Fergusson*, 1983]. The continuation of this axial plane farther to the southeast could possibly be represented by folding in the Hastings Block ("Hastings bend" in Figure 6a), although the link between the two axial plane segments is unclear.

[36] The two-orocline model postulates that deformation in the Manning region was not associated with oroclinal bending, thus explaining the difficulty in observing the curvature of bedding and structural fabrics in this area. If this model is correct, then an alternative structural configuration is required in order to account for rotations and displacements of forearc basin terranes and the apparent folding of the serpentinite belt in the southernmost New England Orogen (Figure 5). For example, in a model suggested by *Collins* [1991], the kinematic evolution of this region was predominantly attributed to faulting and folding during the Hunter-Bowen orogeny (265–230 Ma). However, based on paleomagnetic data [*Geeve et al.*, 2002], it appears that vertical-axis block rotations had occurred earlier (see next section).

[37] The three-orocline model (Figure 3c) is the one that was considered in a number of previous publications [*Cawood and Leitch*, 1985; *Korsch and Harrington*, 1987; *Glen*, 2005; *Klootwijk*, 2009]. It explains the curved pattern of serpentinites and early Permian granitoids in the area of the Manning Orocline (Figure 5). The reason why this curvature is not reflected in the bedding orientations of the (supposedly rotated) forearc basin terranes remains unknown. According to the three-orocline model, the eastern limb of the inferred Nambucca Orocline is the western limb of the Coffs Harbour Orocline [*Korsch*, 1981], meaning that the Nambucca Orocline does not exist (Figure 3c).

[38] The four-orocline model (Figure 3d) explains the spatial distribution of early Permian granitoids (Figure 3d) and is supported by preliminary structural data from the hinge of the Nambucca Orocline [*Moule*, 2011]. A version of this model has recently been discussed by *Cawood et al.* [2011a], who described two doubly vergent pairs of oroclines (Texas-Coffs Harbour and Manning-Hastings).

[39] From a purely geometrical point of view, the complex four-orocline geometry could be explained as an orogenic-scale refolded fold (Figure 6b), in which an earlier steeply plunging or vertical fold (Manning Orocline) was refolded

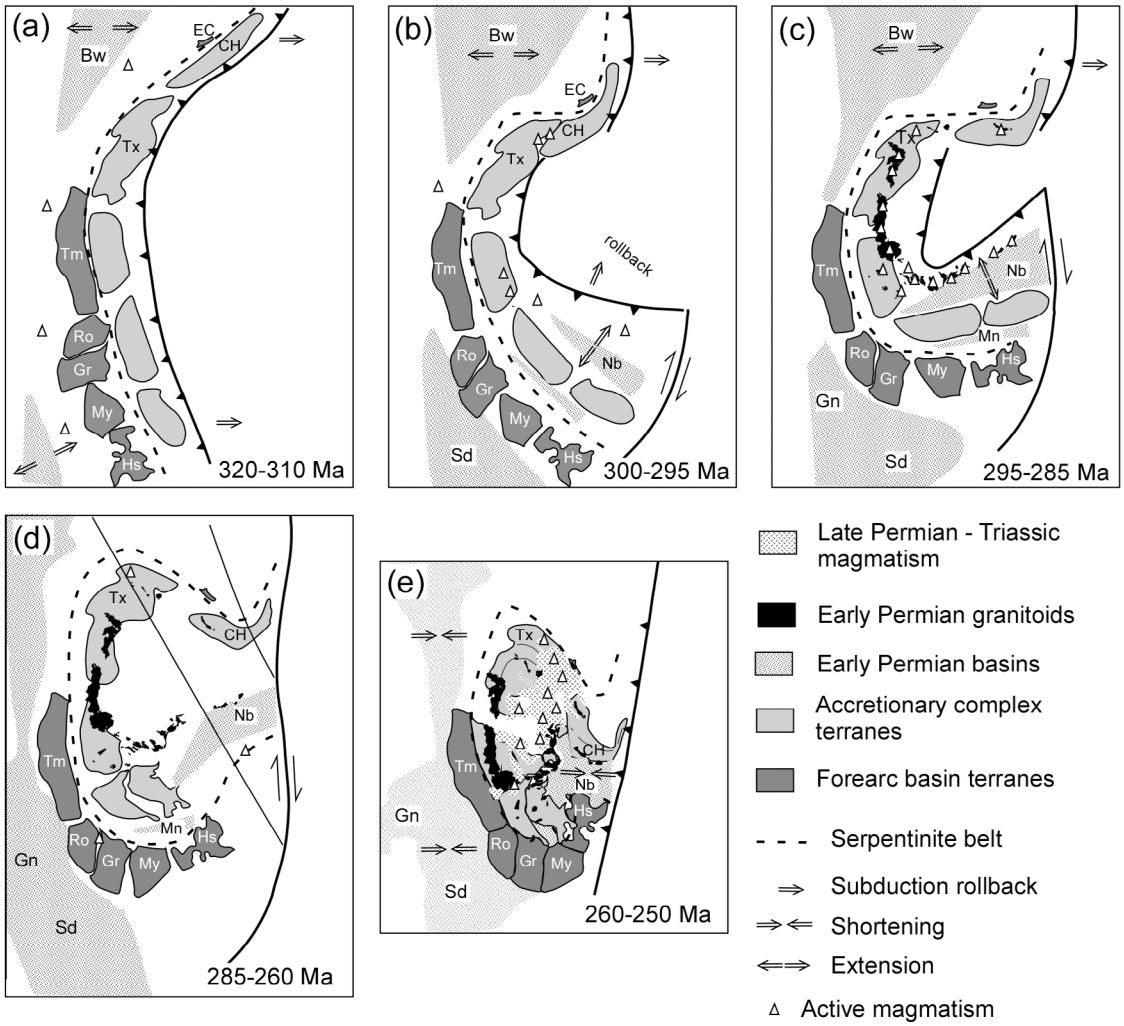

Figure 7. Schematic conceptual model for the development of the New England oroclines. (a) West-dipping subduction in a gently curved Andean-type subduction zone. (b) Subduction rollback leading to slab segmentation in the north and asymmetric backarc extension in the south. (c) Culmination of subduction rollback and the development of the Manning Orocline during wholesale crustal extension. (d) Plate reorganization resulting in the establishment of a dextral transform boundary and associated oroclinal bending in the Texas, Coffs Harbour and Nambucca Oroclines. (e) Reestablishment of an Andean-type subduction zone accompanied by voluminous calc-alkaline magmatism and crustal shortening. Bw, Bowen Basin; CH, Coffs Harbour Block; EC, Emu Creek Block; Gn, Gunnedah Basin; Gr, Gresford Block; Hs, Hastings Block; Mn, Manning Basin; My, Myall Block; Nb, Nambucca Block; Ro, Rouchel Block; Sd, Sydney Basin; Tm, Tamworth Belt; Tx, Texas Block.

around NW-SE axial planes (Texas, Nambucca and Coffs Harbour Oroclines). However, this geometry requires substantial tectonic transports and isoclinal folding of the whole orogenic belt. Therefore, if this model is correct, it has major implications on the tectonic evolution of eastern Australia. Alternatively, one could consider a large-scale interference pattern associated with the superposition of N-S and E-W folds (Figure 6c). This geometry implies that non-cylindrical N-S fold hinges link the Manning and Texas Oroclines, as well as the Coffs Harbour and Nambucca Oroclines. The link between the two latter oroclines, however, does not seem to correspond to the curved pattern of Early Permian granitoids around the Nambucca Oroclines (see question mark in Figure 6c).

6.2. Timing of Oroclinal Bending

[40] Our results indicate that oroclinal bending occurred during and/or after the emplacement of early Permian (296–288 Ma) granitoids and terminated prior to the onset of the second phase of Permian-Triassic (260–230 Ma) magmatism. This second phase of mostly I-type magmatism is characterized by a broadly linear spatial distribution oriented NE-SW, truncating the oroclinal structure (Figure 1).

[41] Time constraints on the development of the Texas and Coffs Harbour Oroclines are based on structural and paleomagnetic data from early Permian rocks [*Aubourg et al.*, 2004; *Li et al.*, 2012]. A conglomerate layer at the base of this rock succession includes volcanic material dated at 293–

291 Ma [*Roberts et al.*, 1996], whereas the youngest strata in this succession are Artinskian (~285–275 Ma [*Briggs*, 1993]). Magnetic fabric data indicate that oroclinal bending commenced prior to deposition of the conglomerate layer, and that a second stage of oroclinal bending continued after the deposition of the overlying sedimentary rocks [*Aubourg et al.*, 2004].

[42] Paleomagnetic data from forearc basin terranes in the Manning Orocline [*Geeve et al.*, 2002] suggest that counterclockwise rotations occurred prior to the Asselian (299–295 Ma). This time constraint, however, should be treated with care, due to the limited paleomagnetic data set and the lack of coeval paleopoles from the different blocks [*Cawood et al.*, 2011a]. If this time constraint is correct, then block rotations occurred prior to the second stage of development of the Texas and Coffs Harbour Orocline, and possibly during the development of extensional rift basins (e.g., Nambucca Block and Manning Basin, Figure 5). An I-type volcanic rock from the base of the Nambucca Block has recently been dated as 292.6 ± 2.0 Ma [*Cawood et al.*, 2011b], i.e., simultaneously with the emplacement of S-type granitoids in the Bundarra and Hillgrove Suites. Given these time constraints, it appears that the curved structure of the early Permian granitoids reflects a primary or a progressive arc (i.e., progressive curvature of the belt during orogenesis [*Weil and Sussman*, 2004]), rather than a secondary bending of an originally linear belt.

[43] Based on the combined structural, geochronological and paleomagnetic data it appears that oroclinal bending occurred in multiple stages. The earlier stage occurred prior or during the development of the early Permian rift system. It involved block rotations in the Manning Orocline, an earlier stage of bending in the Texas and Coffs Harbour Oroclines, and the emplacement of S-type granitoids parallel to the curved structure (i.e., as a primary or progressive arc). The second stage of oroclinal bending is constrained to 285–260 Ma, i.e., after the deposition of the early Permian succession and prior to the onset of the second phase of Permian-Triassic magmatism. This deformation mainly affected the Texas and Coffs Harbour Orocline.

6.3. Tectonic Reconstruction

[44] The complex structure of the New England oroclines has profound implications to tectonic reconstructions of eastern Australia during the Late Paleozoic. Here we propose a conceptual reconstruction model accounting for the development of the four oroclines. We emphasize, however, that all pre-Mesozoic reconstructions are based on patchy data sets and are therefore inevitably incorporating numerous assumptions and potential errors. The aim of our reconstruction, therefore, is only to highlight potential mechanisms that can be tested in future studies.

[45] Previous reconstructions have considered a simpler oroclinal structure, restricted to the Z-shaped geometry of the Texas and Coffs Harbour Oroclines, which was attributed to oblique convergence and dextral strike-slip faulting [*Murray et al.*, 1987; *Offler and Foster*, 2008]. This model could account for the development of the Texas and Coffs Harbour Oroclines, but cannot explain the opposite sense of curvature associated with the Manning Orocline. Furthermore, as recently demonstrated by *Li et al.* [2012], oroclinal bending by dextral strike-slip faulting would impose relatively high strain (>50% shortening) in the area of the Texas Orocline, inconsistently with the observed low strain and the lack of localized shear zones. In our proposed model, therefore, we assume a more complex tectonic history, in which dextral strike-slip faulting is only one stage in the process of oroclinal bending (Figure 7d).

[46] The schematic reconstruction (Figure 7) takes into account the following three mechanisms that are known to generate curvatures in modern orogens: subduction rollback [e.g., *Royden*, 1993; *Schellart et al.*, 2002; *Rosenbaum and Lister*, 2004], strike-slip faulting [e.g., *Kamp*, 1987] and tightening of previous curvatures by bulk shortening.

6.3.1. Subduction Rollback

[47] The reconstruction assumes an originally gently curved shape of the Carboniferous subduction zone (320–310 Ma), similarly to the present-day Bolivian Orocline (Figure 7a). This west-dipping subduction complex was associated with a volcanic arc, a series of forearc basins and a well-developed accretionary wedge. The initial (Carboniferous) orientation of forearc basin terranes (EC, Tm, Gr, Ro, My and Hs in Figure 7a) is back-rotated using information from paleomagnetic data on block rotations around vertical axes (see Section 5). The originally curved structure, particularly in the area of the future Texas Orocline, could be attributed to an inherited bend in the continental margin (e.g., in the boundary between the Lachlan and Thomson Orogens [*Li et al.*, 2012]). Alternatively, it is possible that subduction curvature was attained by the onset of subduction rollback, at 310–305 Ma, in the northern New England Orogen [*Little et al.*, 1992] and in the southern part of the southern New England Orogen [*Jenkins et al.*, 2002], but not in the area in between (Figure 7a). Such variations in rollback velocities along the strike of the subduction zone would result in progressive curvature of the subduction zone, similarly to the way that the Bolivian Orocline may have formed [*Schellart et al.*, 2007].

[48] Subduction rollback in our model is the major mechanism responsible for the formation of the East Australian Rift System in the early Permian. These basins are widest in the north (Bowen Basin) and in the south (Gunnedah and Sydney Basins), but are relatively narrow in the area west of the Tamworth Belt (Figure 7b) [*Korsch et al.*, 2009a]. Accordingly, we propose that in this area the subduction zone was pinned.

[49] We propose that asymmetric subduction rollback in the south was responsible for the formation of the Manning Orocline (Figures 7b and 7c), in a similar way to the modern tectonic evolution of the South Fiji Basin [*Schellart et al.*, 2002]. Oroclinal bending was accompanied by backarc extension, giving rise to the development of the early Permian rift basins in the Nambucca Block and Manning Basin (Figure 7b). A relatively early (~300–290 Ma) development of the Manning Orocline is supported by paleomagnetic data, which suggest a minimum age of counterclockwise rotations in the Asselian (299–295 Ma) [*Geeve et al.*, 2002; *Klootwijk*, 2009]. It also explains the distinctly different structural and metamorphic history recorded in the area of the Manning Orocline in comparison with the deformation around the three other oroclines.

[50] North of the pinning zone, eastward rollback resulted in widespread extension, involving the development of grabens and half grabens [*Holcombe et al.*, 1997a]. We propose

that subduction rollback north of the pinning zone resulted in the segmentation of the subduction zone, giving rise to the emplacement of relatively small plutons with heterogeneous composition, including both S- and I-type granitoids and some mafic components (e.g., Mt You You Suite). In contrast, magmatism in the area opposite the pinned subduction segment was characterized by the voluminous S-type Bundarra Granite and was much more homogenous (Figure 7c).

6.3.2. Plate Boundary Reorganization

[51] Only minor magmatism occurred in the period from 285 Ma to 260 Ma (Figure 2), and this is interpreted as indicating plate reorganization and a temporal cessation of subduction processes. The reconstruction follows previous suggestions for oblique convergence and a dextral transform boundary [*Murray et al.*, 1987; *Offler and Foster*, 2008], responsible for oroclinal bending in the Texas, Coffs Harbour and Nambucca Oroclines (Figure 7d). A local collision between the early Permian Nambucca Block and the Coffs Harbour Block was possibly responsible for the development of penetrative deformation within the early Permian sedimentary rocks at 264–260 Ma [*Offler and Foster*, 2008].

6.3.3. Hunter-Bowen Orogeny

[52] The final stage in the development of the New England oroclines involved tightening by E-W shortening (Figure 7e). This tectonic episode is attributed to the Hunter-Bowen orogeny, which commenced at ~265 Ma and was associated with folding and thrusting [*Collins*, 1991; *Holcombe et al.*, 1997b; *Korsch et al.*, 2009b]. Regional contractional deformation has also affected the early Permian Sydney-Gunnedah Basins, and was responsible for the development of overprinting N-S structural fabric in the Nambucca Block [*Johnston et al.*, 2002]. Deformation was accompanied by widespread calc-alkaline magmatism, indicating that an Andean-type subduction zone was reestablished.

7. Conclusions

[53] In this paper, we presented 19 new U-Pb zircon ages from early Permian granitoids in the southern New England Orogen. All ages, except of one, are clustered at 296–288 Ma consistently with other recently published geochronological data [*Cawood et al.*, 2011b]. The new time constraints on granite emplacement enable us to recognize a continuous belt of early Permian granitoids that define a complex oroclinal structure.

[54] The recognition of a contorted belt of early Permian granitoids and rift sequences highlights the geometry of the New England oroclines. We propose that the early Permian magmatic belt is curved along the Manning Orocline (Figure 3), thus supporting earlier suggestions on the existence of this orocline [*Cawood and Leitch*, 1985; *Korsch and Harrington*, 1987]. Furthermore, we propose the existence of a fourth oroclinal structure, the Nambucca Orocline, which appears as the refolded eastern limb of the Manning orocline (Figure 7d). Future structural and paleomagnetic studies should test the proposed quadruple oroclinal geometry, which appears as one of the most complex contorted orogens worldwide.

[55] The geodynamic setting responsible for the formation of this oroclinal structure remains speculative. We propose a conceptual model, involving an early development of the Manning Orocline by asymmetric subduction rollback, followed by oroclinal bending by dextral traspression, and tightening of the oroclines by a subsequent event of regional E-W shortening.

[56] **Acknowledgments.** This work was funded by the Australian Research Council (DP0986762). The manuscript benefited from comments by A. Yonkee and two anonymous reviewers. We also thank R. Offler, R. Korsch, S. Johnston, R. Holcombe, and R Weinberg for providing comments on earlier versions of this manuscript. P. Nuriel is thanked for assisting with the illustrations.

References

Abrajevitch, A., R. Van der Voo, N. M. Levashova, and M. L. Bazhenov (2007), Paleomagnetic constraints on the paleogeography and oroclinal bending of the Devonian volcanic arc in Kazakhstan, *Tectonophysics*, *441*, 67–84, doi:10.1016/j.tecto.2007.04.008.

Asthana, D., and E. C. Leitch (1985), Petroi metabasalt: Alkaline within-plate mafic rocks from the Nambucca slate belt, northeastern New South Wales, *Aust. J. Earth Sci.*, *32*(3), 261–277, doi:10.1080/08120098508729329.

Aubourg, C., C. Klootwijk, and R. J. Korsch (2004), Magnetic fabric constraints on oroclinal bending of the Texas and Coffs Harbour blocks: New England Orogen, eastern Australia, in *Magnetic Fabric: Methods and Applications*, edited by F. Martín-Hernández et al., *Geol. Soc. Spec. Publ.*, *238*, 421–445.

Binns, R. A., B. W. Chappell, R. H. Flood, R. J. Gunthorpe, E. Hobson, M. J. Neilson, J. E. Ransley, and M. J. Slade (1967), Geological Map of New England, 1:250,000—New England Tableland, Southern Part, with explanatory text, map, Univ. of New England, Armidale, N. S. W., Australia.

Black, L. P., S. L. Kamo, C. M. Allen, J. M. Aleinikoff, D. W. Davis, R. J. Korsch, and C. Foudoulis (2003), TEMORA 1: A new zircon standard for Phanerozoic U-Pb geochronology, *Chem. Geol.*, *200*, 155–170, doi:10.1016/S0009-2541(03)00165-7.

Briggs, D. J. C. (1993), Time Control in the Permian of the New England Orogen, paper presented at New England Orogen, eastern Australia, Dep. of Geol. and Geophys., Univ. of N. Engl., Armidale.

Bryant, C. J., R. J. Arculus, and B. W. Chappell (1997a), Clarence River Supersuite: 250 Ma Cordilleran tonalitic I-type intrusions in eastern Australia, *J. Petrol.*, *38*(8), 975–1001, doi:10.1093/petrology/38.8.975.

Bryant, C. J., M. A. Cosca, and R. J. Arculus (1997b), $^{40}Ar/^{39}Ar$ ages of Clarence River Supersuite intrusions from the northern portion of the New England Batholith, southern New England Orogen, in *Tectonics and Metallogenesis of the New England Orogen*, edited by P. M. Ashley and P. G. Flood, *Spec. Publ. Geol. Soc. Aust.*, *19*, 52–65.

Caprarelli, G., and E. C. Leitch (2001), Geochemical evidence from Lower Permian volcanic rocks of northeast New South Wales for asthenospheric upwelling following slab breakoff, *Aust. J. Earth Sci.*, *48*, 151–166, doi:10.1046/j.1440-0952.2001.00850.x.

Carey, S. W. (1955), The orocline concept in geotectonics, *Pap. Proc. R. Soc. Tasmania*, *89*, 255–288.

Cawood, P. A. (1982), Structural relations in the subduction complex of the Paleozoic New England fold belt, eastern Australia, *J. Geol.*, *90*(4), 381–392, doi:10.1086/628692.

Cawood, P. A., and E. C. Leitch (1985), Accretion and dispersal tectonics of the Southern New England Fold Belt, Eastern Australia, in *Tectonostratigraphic Terranes of the Circum-Pacific Region*, *Earth Sci. Ser.*, vol. 1, edited by D. G. Howell, pp. 481–492, Circum-Pac. Counc. for Energy and Miner. Resour., Houston, Tex.

Cawood, P. A., S. A. Pisarevsky, and E. C. Leitch (2011a), Unraveling the New England orocline, east Gondwana accretionary margin, *Tectonics*, *30*, TC5002, doi:10.1029/2011TC002864.

Cawood, P. A., E. C. Leitch, R. E. Merle, and A. Nemchin (2011b), Orogenesis without collision: Stabilizing the Terra Australis accretionary orogen, eastern Australia, *Geol. Soc. Am. Bull.*, *123*, 2240–2255, doi:10.1130/B30415.1.

Cifelli, F., M. Mattei, and F. Rossetti (2007), Tectonic evolution of arcuate mountain belts on top of a retreating subduction slab: The example of the Calabrian Arc, *J. Geophys. Res.*, *112*, B09101, doi:10.1029/2006JB004848.

Collins, W. J. (1991), A reassessment of the "Hunter-Bowen orogeny": tectonic implications for the southern New England fold belt, *Aust. J. Earth Sci.*, *38*(4), 409–423, doi:10.1080/08120099108727981.

Collins, W. J., and S. W. Richards (2008), Geodynamic significance of S-type granites in circum-Pacific orogens, *Geology*, *36*(7), 559–562, doi:10.1130/G24658A.1.

Collins, W. J., R. Offler, T. R. Farrell, and B. Landenberger (1993), A revised Late Palaeozoic–Early Mesozoic tectonic history for the southern New England Fold Belt, paper presented at New England Orogen, eastern Australia, Dep. of Geol. and Geophys., Univ. of N. Engl., Armidale, N. S. W., Australia.

Crook, K. A. W. (1964), Depositional environmental and provenance of Devonian and Carboniferous sediments in the Tamworth Trough, N.S.W, *J. Proc. R. Soc. N. S. W.*, *97*, 41–53.

Cross, K. C., C. L. Fergusson, and P. G. Flood (1987), Contrasting structural styles in the Paleozoic subduction complex of the Southern New England Orogen, Eastern Australia, in *Terrane Accretion and Orogenic Belts*, *Geodyn. Ser.*, vol. 19, edited by E. Leitch and E. Scheibner, pp. 83–92, AGU, Washington, D. C., doi:10.1029/GD019p0083.

Cross, A. J., D. J. Purdy, R. J. Bultitude, C. R. Dhnaram, and F. E. von Gnielinski (2009), Joint GSQ-GA NGA geochronology project, New England Orogen and Drummond Basin, in *Queensland Geological Record, 2009/03*, report, Dep. of Employment, Econ. Dev., and Innovation, Queensl. Gov., City East, Queensl., Australia.

Dirks, P. H. G. M., M. Hand, W. J. Collins, and R. Offler (1992), Structural-metamorphic evolution of the Tia complex, New England fold belt; thermal overprint of an accretion-subduction complex in a compressional back-arc setting, *J. Struct. Geol.*, *14*(6), 669–688, doi:10.1016/0191-8141(92)90125-G.

Dirks, P. H. G. M., R. Offler, and W. J. Collins (1993), Timing of emplacement and deformation of the Tia Granodiorite, southern New England Fold Belt, NSW: Implications for the metamorphic history, *Aust. J. Earth Sci.*, *40*(2), 103–108, doi:10.1080/08120099308728067.

Donchak, P. J. T., R. J. Bultitude, D. J. Purdy, and T. J. Denaro (2007), Geology and mineralisation of the Texas Region, south-eastern Queensland, in *Queensland Geology*, *11*, report, Dep. of Employment, Econ. Dev., and Innovation, Queensl. Gov., City East, Queensl., Australia.

Fergusson, C. L. (1984), Tectono-stratigraphy of a Palaeozoic subduction complex in the central Coffs Harbour Block of north-eastern New South Wales, *Aust. J. Earth Sci.*, *31*, 217–236, doi:10.1080/08120098408729293.

Fergusson, C. L. (1991), Thin-skinned thrusting in the northern New England orogen, central Queensland, Australia, *Tectonics*, *10*, 797–806, doi:10.1029/90TC02708.

Flood, R. H., and S. E. Shaw (1975), A cordierite-bearing granite suite from the New England Batholith, N.S.W., Australia, *Contrib. Mineral. Petrol.*, *52*(3), 157–164, doi:10.1007/BF00457291.

Flood, R. H., and S. E. Shaw (1977), Two "S-type" granite suites with low initial $^{87}Sr/^{86}Sr$ ratios from the New England Batholith, Australia, *Contrib. Mineral. Petrol.*, *61*(2), 163–173, doi:10.1007/BF00374365.

Fukui, S., T. Watanabe, T. Ithaya, and E. C. Leitch (1995), Middle Ordovician high PT metamorphic rocks in eastern Australia: Evidence from K-Ar ages, *Tectonics*, *14*, 1014–1020, doi:10.1029/94TC01317.

Geeve, R. J., P. W. Schmidt, and J. Roberts (2002), Paleomagnetic results indicate pre-Permian counter-clockwise rotation of the southern Tamworth Belt, southern New England Orogen, Australia, *J. Geophys. Res.*, *107*(B9), 2196, doi:10.1029/2000JB000037.

Ghiglione, M. C., and E. O. Cristallini (2007), Have the southernmost Andes been curved since Late Cretaceous time? An analog test for the Patagonian Orocline, *Geology*, *35*(1), 13–16, doi:10.1130/G22770A.1.

Glen, R. A. (2005), The Tasmanides of eastern Australia, in *Terrane Processes at the Margins of Gondwana*, edited by A. P. M. Vaughan, P. T. Leat, and R. J. Pankhurst, *Geol. Soc. Spec. Publ.*, *246*, 23–96.

Graham, I. J., and R. J. Korsch (1985), Rb-Sr geochronology of coarse-grained greywackes and argillites from the coffs harbour block, Eastern Australia, *Chem. Geol.*, *58*(1–2), 45–54, doi:10.1016/0168-9622(85)90026-0.

Gutiérrez-Alonso, G., J. Fernández-Suárez, A. B. Weil, J. B. Murphy, R. D. Nance, F. Corfú, and S. T. Johnston (2008), Self-subduction of the Pangaean global plate, *Nat. Geosci.*, *1*, 549–553, doi:10.1038/ngeo250.

Holcombe, R. J., C. J. Stephens, C. R. Fielding, D. Gust, T. A. Little, R. Sliwa, J. McPhie, and A. Ewart (1997a), Tectonic evolution of the northern New England Fold Belt: Carboniferous to Early Permian transition from active accretion to extension, in *Tectonics and Metallogenesis of the New England Orogen*, edited by P. M. Ashley and P. G. Flood, *Spec. Publ. Geol. Soc. Aust.*, *19*, 66–79.

Holcombe, R. J., C. J. Stephens, C. R. Fielding, D. Gust, T. A. Little, R. Sliwa, J. McPhie, and A. Ewart (1997b), Tectonic evolution of the northern New England Fold Belt: The Permian-Triassic Hunter-Bowen event, in *Tectonics and metallogenesis of the New England Orogen*, edited by P. M. Ashley and P. G. Flood, *Spec. Publ. Geol. Soc. Aust.*, *19*, 52–65.

Jenkins, R. B., B. Landenberger, and W. J. Collins (2002), Late Palaeozoic retreating and advancing subduction boundary in the New England Fold Belt, New South Wales, *Aust. J. Earth Sci.*, *49*(3), 467–489, doi:10.1046/j.1440-0952.2002.00932.x.

Johnston, S. T. (2001), The great Alaskan terrane wreck; reconciliation of paleomagnetic and geological data in the northern Cordillera, *Earth Planet. Sci. Lett.*, *193*(3–4), 259–272, doi:10.1016/S0012-821X(01)00516-7.

Johnston, S. T., and S. Mazzoli (2009), The Calabrian Orocline: Buckling of a previously more linear orogen, in *Ancient Orogens and Modern Analogues*, edited by J. B. Murphy, J. D. Keppie and A. J. Hynes, *Geol. Soc. Spec. Publ.*, *327*, 113–125.

Johnston, A. J., R. Offler, and S. Liu (2002), Structural fabric evidence for indentation tectonics in the Nambucca Block, southern New England Fold Belt, New South Wales, *Aust. J. Earth Sci.*, *49*(2), 407–421, doi:10.1046/j.1440-0952.2002.00919.x.

Kamp, P. J. J. (1987), Age and origin of the New Zealand Orocline in relation to Alpine Fault movement, *J. Geol. Soc.*, *144*(4), 641–652, doi:10.1144/gsjgs.144.4.0641.

Kastens, K., et al. (1988), ODP leg 107 in the Tyrrhenian Sea: Insights into passive margin and back-arc basin evolution, *Geol. Soc. Am. Bull.*, *100*(7), 1140–1156, doi:10.1130/0016-7606(1988)100<1140:OLITTS>2.3.CO;2.

Kent, A. J. R. (1994), Geochronology and geochemistry of Palaeozoic intrusive rocks in the Rockvale region, southern New England Orogen, New South Wales, *Aust. J. Earth Sci.*, *41*(4), 365–379, doi:10.1080/08120099408728145.

Kent, D. V. (1988), Further paleomagnetic evidence for oroclinal rotation in the central folded Appalachians from the Bloomsburg and Mauch Chunk formations, *Tectonics*, *7*, 749–759, doi:10.1029/TC007i004p00749.

Kleeman, J. D., I. R. Plimer, J. Lu, D. A. Foster, and R. Davidson (1997), Timing of thermal and mineralisation events associated with the Mole Granite, in *Tectonics and Metallogenesis of the New England Orogen*, edited by P. M. Ashley and P. G. Flood, *Spec. Publ. Geol. Soc. Aust.*, *19*, 254–265.

Klootwijk, C. (2009), Sedimentary basins of eastern Australia: Paleomagnetic constraints on geodynamic evolution in a global context, *Aust. J. Earth Sci.*, *56*(3), 273–308, doi:10.1080/08120090802695741.

Korsch, R. J. (1981), Deformational history of the Coffs Harbour Block, *J. Proc. R. Soc. N. S. W.*, *114*, 17–22.

Korsch, R. J., and H. J. Harrington (1987), Oroclinal bending, fragmentation and deformation of terranes in the New England Orogen, eastern Australia, in *Terrane Accretion and Orogenic Belts*, *Geodyn. Ser*, vol. 19, edited by E. C. Leitch and E. Scheibner, pp. 129–139, AGU, Washington, D. C., doi:10.1029/GD019p0129.

Korsch, R. J., N. R. Archer, and G. W. McConachy (1978), The Demon Fault, *J. Proc. R. Soc. N. S. W.*, *111*, 101–106.

Korsch, R. J., J. M. Totterdell, D. L. Cathro, and M. G. Nicoll (2009a), Early Permian East Australian Rift System, *Aust. J. Earth Sci.*, *56*(3), 381–400, doi:10.1080/08120090802698703.

Korsch, R. J., J. M. Totterdell, T. Fomin, and M. G. Nicoll (2009b), Contractional structures and deformational events in the Bowen, Gunnedah and Surat Basins, eastern Australia, *Aust. J. Earth Sci.*, *56*(3), 477–499, doi:10.1080/08120090802698745.

Leitch, E. C. (1974), The geological development of the southern part of the New England Fold Belt, *J. Geol. Soc. Aust.*, *21*, 133–156.

Leitch, E. (1988), The Barnard Basin and the early Permian development of the southern part of the New England Fold Belt, in *New England Orogen: Tectonics and Metallogenesis*, edited by J. D. Kleeman, pp. 61–67, Univ. of N. Engl., Armidale, N. S. W., Australia.

Leitch, E. C., and P. A. Cawood (1980), Olistoliths and debris flow deposits at ancient consuming plate margins: An eastern Australian example, *Sediment. Geol.*, *25*(1–2), 5–22, doi:10.1016/0037-0738(80)90051-2.

Lennox, P. G., and P. G. Flood (1997), Age and structural characterisation of the Texas megafold, southern New England Orogen, eastern Australia, in *Tectonics and Metallogenesis of the New England Orogen*, edited by P. M. Ashley and P. G. Flood, *Spec. Publ. Geol. Soc. Aust.*, *19*, 161–177.

Lennox, P. G., and J. Roberts (1988), The Hastings Block - a key to the tectonic development of the New England Orogen, in *New England Orogen: Tectonics and Metallogenesis*, edited by J. D. Kleeman, pp. 68–77, Univ. of N. Engl., Armidale, N. S. W., Australia.

Li, P., G. Rosenbaum, and P. J. T. Donchak (2012), Structural evolution of the Texas Orocline, eastern Australia, *Gondwana Res.*, in press.

Little, T. A., R. J. Holcombe, G. M. Gibson, R. Offler, P. B. Gans, and M. O. McWilliams (1992), Exhumation of late Paleozoic blueschists in Queensland, Australia, by extensional faulting, *Geology*, *20*(3), 231–234, doi:10.1130/0091-7613(1992)020<0231:EOLPBI>2.3.CO;2.

Lonergan, L., and N. White (1997), Origin of the Betic-Rif mountain belt, *Tectonics*, *16*, 504–522, doi:10.1029/96TC03937.

Ludwig, K. R. (2003), Isoplot 3.00: A geochronological toolkit for Microsoft Excel, *Berkeley Geochronol. Cent. Spec. Publ. 4*, 70 pp., Berkeley Geochronol. Cent., Berkeley, Calif.

Mantovani, E., D. Albarello, C. Tamburelli, and D. Babbucci (1996), Evolution of the Tyrrhenian basin and surrounding regions as a result of the Africa-Eurasia convergence, *J. Geodyn.*, *21*(1), 35–72, doi:10.1016/0264-3707(95)00011-9.

Marshak, S. (1988), Kinematics of orocline and arc formation in thin-skinned orogens, *Tectonics*, *7*, 73–86, doi:10.1029/TC007i001p00073.

Marshak, S. (2004), Salients, recesses, arcs, oroclines, and syntaxes: A review of ideas concerning the formation of map-view curves in fold-thrust belts, in *Thrust Tectonics and Hydrocarbon Systems*, *AAPG Mem.*, vol. 82, edited by K. R. McClay, pp. 131–156, Am. Assoc. of Pet. Geol., Tulsa, Okla.

McPhie, J. (1987), Andean analogue for Late Carboniferous volcanic arc and arc flank environments of the western New England Orogen, New South Wales, Australia, *Tectonophysics*, *138*, 269–288, doi:10.1016/0040-1951(87)90044-8.

McPhie, J., and C. L. Fergusson (1983), Dextral movement on the Demon Fault, northeastern New South Wales: A reassessment (Australia), *J. Proc. R. Soc. N. S. W.*, *116*(3–4), 123–127.

Mensel, H. D., M. T. McCulloch, and B. W. Chappell (1985), The New England Batholith: Constraints on its derivation from Nd and Sr isotopic studies of granitoids and country rocks, *Geochim. Cosmochim. Acta*, *49*, 369–384, doi:10.1016/0016-7037(85)90030-4.

Milligan, P. R., R. Franklin, B. R. S. Minty, L. M. Richardson, and P. J. Percival (2010), Magnetic Anomaly Map of Australia (Fifth Edition), scale 1:5,000,000, map, Geosci. Aust., Canberra.

Moule, E. (2011), Structure and deformation of the Henry River area east of Glen Innes, north-eastern New South Wales, BS thesis, 185 pp., School of Earth Sci., Univ. of Queensl., Brisbane, Queensl., Australia.

Murray, C. G., C. L. Fergusson, P. G. Flood, W. G. Whitaker, and R. J. Korsch (1987), Plate tectonic model for the Carboniferous evolution of the New England Fold Belt (Australia), *Aust. J. Earth Sci.*, *34*(2), 213–236, doi:10.1080/08120098708729406.

Offler, R., and D. A. Foster (2008), Timing and development of oroclines in the southern New England Orogen, New South Wales, *Aust. J. Earth Sci.*, *55*(3), 331–340, doi:10.1080/08120090701769464.

Roberts, J., and B. A. Engel (1987), Depositional and tectonic history of the southern New England orogen, *Aust. J. Earth Sci.*, *34*(1), 1–20, doi:10.1080/08120098708729391.

Roberts, J., J. C. Claoué-Long, and C. B. Foster (1996), SHRIMP zircon dating of the Permian System of eastern Australia, *Aust. J. Earth Sci.*, *43*(4), 401–421, doi:10.1080/08120099608728264.

Rosenbaum, G. (2010), Structure of the New England oroclines, in *New England Orogen 2010 Conference Proceedings*, edited by S. Buckman and P. L. Blevin, pp. 297–302, Univ. of N. Engl., Armidale, N. S. W., Australia.

Rosenbaum, G. (2012), The oroclines of the southern New England Orogen, eastern Australia, *Episodes*, in press.

Rosenbaum, G., and G. S. Lister (2004), Formation of arcuate orogenic belts in the western Mediterranean region, in *Orogenic Curvature: Integrating Paleomagnetic and Structural Analyses*, edited by A. J. Sussman and A. B. Weil, *Spec. Pap. Geol. Soc. Am.*, *383*, 41–56.

Rosenbaum, G., M. Gasparon, F. P. Lucente, A. Peccerillo, and M. S. Miller (2008), Kinematics of slab tear faults during subduction segmentation and implications for Italian magmatism, *Tectonics*, *27*, TC2008, doi:10.1029/2007TC002143.

Royden, L. H. (1993), Evolution of retreating subduction boundaries formed during continental collision, *Tectonics*, *12*, 629–638, doi:10.1029/92TC02641.

Schellart, W. P., G. S. Lister, and M. W. Jessell (2002), Analogue modeling of arc and backarc deformation in the New Hebrides Arc and North Fiji Basin, *Geology*, *30*(4), 311–314, doi:10.1130/0091-7613(2002)030<0311:AMOAAB>2.0.CO;2.

Schellart, W. P., J. Freeman, D. R. Stegman, L. Moresi, and D. May (2007), Evolution and diversity of subduction zones controlled by slab width, *Nature*, *446*, 308–311, doi:10.1038/nature05615.

Schmidt, P. W., C. Aubourg, P. G. Lennox, and J. Roberts (1994), Palaeomagnetism and tectonic rotation of the Hastings Terrane, eastern Australia, *Aust. J. Earth Sci.*, *41*(6), 547–560, doi:10.1080/08120099408728165.

Shaw, S. E. (1994), Late Permian-Triassic radiometric dates of granitoids and associated volcanics from the southern New England belt, in *Permian-Triassic Pangean Basins and Foldbelts Along the Panthalassan Margin of Gondwanaland*, edited by J. Veevers and C. M. Powell, *Mem. Geol. Soc. Am.*, *184*, 147–159.

Shaw, S. E., and R. H. Flood (1981), The New England batholith, eastern Australia: Geochemical variations in time and space, *J. Geophys. Res.*, *86*(B11), 10,530–10,544, doi:10.1029/JB086iB11p10530.

Stacey, J. S., and J. D. Kramers (1975), Approximation of terrestrial lead isotope evolution by a two-stage model, *Earth Planet. Sci. Lett.*, *26*, 207–221, doi:10.1016/0012-821X(75)90088-6.

Sussman, A. J., and A. B. Weil (Eds.) (2004), *Orogenic Curvature: Integrating Paleomagnetic and Structural Analyses*, *Spec. Pap. Geol. Soc. Am.*, *383*, 271 pp.

Van der Voo, R. (2004), Paleomagnetism, oroclines, and growth of the continental crust, *GSA Today*, *14*(12), 4–9, doi:10.1130/1052-5173(2004)014<4:POAGOT>2.0.CO;2.

Vickery, N. M., P. M. Ashley, and C. M. Fanning (1997), Dumboy-Gragin Granite, northeastern New South Wales: Age and compositional affinities, in *Tectonics and Metallogenesis of the New England Orogen*, edited by P. M. Ashley and P. G. Flood, *Spec. Publ. Geol. Soc. Aust.*, *19*, 266–271.

Weil, A. B., and A. J. Sussman (2004), Classifying curved orogens based on timing relationships between structural development and vertical-axis rotations, in *Orogenic Curvature: Integrating Paleomagnetic and Structural Analyses*, edited by A. J. Sussman and A. B. Weil, *Spec. Pap. Geol. Soc. Am.*, *383*, 1–15.

Weil, A. B., R. Van der Voo, B. A. van der Pluijm, and J. M. Parés (2000), The formation of an orocline by multiphase deformation: A paleomagnetic investigation of the Cantabria–Asturias Arc (northern Spain), *J. Struct. Geol.*, *22*, 735–756, doi:10.1016/S0191-8141(99)00188-1.

Weil, A. B., R. Van der Voo, and B. A. van der Pluijm (2001), Oroclinal bending and evidence against the Pangea megashear: The Cantabria-Asturias arc (northern Spain), *Geology*, *29*(11), 991–994, doi:10.1130/0091-7613(2001)029<0991:OBAEAT>2.0.CO;2.

Weil, A. B., A. Yonkee, and A. Sussman (2010), Reconstructing the kinematic evolution of curved mountain belts: A paleomagnetic study of Triassic red beds from the Wyoming salient, Sevier thrust belt, U.S, *Geol. Soc. Am. Bull.*, *122*(1–2), 3–23, doi:10.1130/B26483.1.

Williams, I. S. (1998), U-Th-Pb geochronology by ion microprobe, in *Applications of Microanalytical Techniques to Understanding Mineralizing Processes*, *Rev. Econ. Geol.*, vol. 7, edited by M. A. McKibben, W. C. P. Shanks, and W. I. Ridley, pp. 1–35, Soc. of Econ. Geol., Littleton, Colo.

Xiao, W., B. Huang, C. Han, S. Sun, and J. Li (2010), A review of the western part of the Altaids: A key to understanding the architecture of accretionary orogens, *Gondwana Res.*, *18*(2–3), 253–273, doi:10.1016/j.gr.2010.01.007.

P. Li and G. Rosenbaum, School of Earth Sciences, University of Queensland, Brisbane, QLD 4072, Australia. (g.rosenbaum@uq.edu.au)

D. Rubatto, Research School of Earth Sciences, Australian National University, Mills Road, Canberra, ACT 0200, Australia.